Journal of the Mechanical Behavior of Biomedical Materials 90 (2019) 615–625

Contents lists available at ScienceDirect

Journal of the Mechanical Behavior of Biomedical Materials

journal homepage: www.elsevier.com/locate/jmbbm

Optimization method for the determination of Mooney-Rivlin material coefficients of the human breasts in-vivo using static and dynamic finite element models

Yue Sun[a], Lihua Chen[b], Kit-lun Yick[a,*], Winnie Yu[a], Newman Lau[c], Wanzhong Jiao[a]

[a] Institute of Textiles and Clothing, The Hong Kong Polytechnic University, Hong Kong
[b] College of Mechanical Engineering, Beijing University of Technology, Beijing, PR China
[c] School of Design, The Hong Kong Polytechnic University, Hong Kong

ARTICLE INFO

Keywords:
Finite element method
Forward-leaning
Breast deformation
Material property
Hyperelastic

ABSTRACT

It has been a long-standing problem in the engineering design of bra for optimal support and shaping due to the difficulty of quantifying the hyper-elastic properties of human breasts. The objective of this study is to determine an optimal approach to obtain the non-linear properties of breast soft tissues and the corresponding deformations during motions. The Mooney-Rivlin material parameters of the breasts in-vivo were verified through an optimization process that involved iteratively changing the material coefficients with the integration of static and dynamic finite element models. Theoretical equations of a rigid-flexible coupled system during the motion of forward-leaning were established with gravitational, centrifugal and Coriolis forces to simulate the dynamic deformation of the flexible breasts. The resultant, optimally generated, coefficients of the Mooney-Rivlin hyperelastic material type for the breast were found. This new set of breast material coefficients was verified by finite element analysis of the breast deformation during forward-leaning and running movement. The method proposed in this study provides an effective way to determine the breast properties for predicting breast deformation and analysis of the bra-breast contact mechanism and thus, improving the design of bras.

1. Introduction

The breast has an inhomogeneous structure including various parts with different constructions and material properties (Ramião et al., 2016). The predominant parts of the breast include adipose tissue, glandular tissue, and the skin, which their mechanical properties diverse in a large range resulting from different ages and genetic factors (Poplack et al., 2004). Patient-specific biomechanical model of the breast with computer-aided analysis in different positions to reflect the sequence of deformation images of the soft tissues has been previously studied for clinical diagnoses (Schnabel et al., 2003). The simulation results of breast deformation have also been used for the outcome prediction in plastic surgeon (Sutradhar and Miller, 2013). Nevertheless, the mechanical properties of soft breast play a vital part in the construction and accuracy of such models. In the apparel industry, the level of breast support, shape and comfort are major concerns in bra design and development. However, the contact mechanics between a bra and breast soft tissues are highly complex. The subject-specific material properties of breast and their biomechanical interactions with a bra are of an increasing interest to enhance the breast support and shaping for optimal design of bras (Zain-Ul-Abdein et al., 2013).

Traditionally, breast properties have been measured ex-vivo by an indentation test on the small “dead” fatty and glandular tissues collected and segmented after breast surgery (Krouskop, 1998; Omidi et al., 2014; Samani et al., 2003; Samani et al., 2004). In-vivo measurements have been obtained by ultrasonic scanning of the soft tissues under the skin, or by applying a small deformation to the soft tissues (Han et al., 2003; Skovoroda, 1994). Both methods can reflect only the elastic property of the material. However, the hyperelastic breast material, which exhibits nonlinear behavior during large deformation movement, is better represented by Mooney-Rivlin coefficients (Eder et al., 2014). With the advances of simulation techniques, finite element method is broadly applied to analyse problems associated with biomechanics (Del Palomar et al., 2008). This method is not only able to predict the hyper elastic properties of the breast tissue with consideration of the ex-vivo measurement, but also able to be used alongside the imaging registration method. A biomechanical model of the breast is built by finite element method to predict deformations

* Corresponding author.
E-mail address: kit-lun.yick@polyu.edu.hk (K.-l. Yick).

https://doi.org/10.1016/j.jmbbm.2018.11.016
Received 16 April 2018; Received in revised form 2 November 2018; Accepted 18 November 2018
Available online 22 November 2018
1751-6161/ © 2018 The Authors. Published by Elsevier Ltd. This is an open access article under the CC BY-NC-ND license (http://creativecommons.org/licenses/BY-NC-ND/4.0/).

when applying external loading (e.g. gravity or compression). The resulting shape is compared with the real state breast images using identified landmarks and 3D scanner images, thus optimizing the material parameters to make the two images correlate with each other.

Dufaye (2013) built an FE deformable breast model with linear material properties to simulate nipple displacement which was validated experimentally. Gravity force was applied to the breasts and then the nipple position was compared with the geometry of a deformable breast from MRI data. However, such linear FE model cannot predict large deformation of breasts. Eder et al. (2014) initially constructed a gravity-free breast model from MRI data, and then the simulated breast shape in a standing upright position was compared with actual 3-D scans of the body surface. Amongst the 12 reviewed material models from previous publications, the Neo-Hookean hyperelastic models proposed by Tanner et al. (2006) (C_{10} = 0.13 kPa) and Rajagopal et al. (2008) (C_{10} = 0.08 kPa) produce the most appropriate material coefficients. However, only static imaging registration of the breast shapes in two body postures was compared within the 12 discrete material parameters. The second author of this paper, Chen et al. (Chen et al., 2013) previously conducted a study of breast material property based on numerical simulation method. A dynamic breast model using hyperelastic neoHookean material was developed to simulate the large deformations in the breasts during three activities and validated the results with motion capture experimental data. Recently, the research team (Cai et al., 2018) used a piecewise mass-spring-damper model to calculate the viscous damping ratio in-vivo during the free-falling of the breasts and found that this material property varies under the different phases of breast movement. These studies have laid the foundation knowledge of the non-linear properties of breast tissues and derived the shear modulus and viscous damping ratio of breast material, but the hyper-elastic material parameters have not yet been defined.

Considering the limitations of the previous work, this study was the first attempt to combine the static and dynamic FE models of the breasts in-vivo and used iterative changes to the nonlinear Mooney-Rivlin breast material coefficients to simulate the large deformations exhibited by the breast during forward-leaning motion. The key contribution of developing a dynamic biomechanical model of breast associating with a static model in this study is its high efficiency of searching the optimal solution to the hyper-elastic material properties and high accuracy to predict the breast deformation during motions rather than two states of breast profiles used in image registration.

2. Materials and methods

The principal feature of this paper is the static and dynamic FE models to determine the breast material parameters. Before developing the FE model, a geometric body model was developed based on a 3D-scan image of the subject's body surface. A meshed model of the upper torso part was created for FE modeling. Then, iterative sets of nonlinear material coefficients were input into the FE model to simulate breast deformation at different angles of forward-leaning. The simulated results were compared with the data obtained from motion capture analysis.

2.1. Experiments

2.1.1. Subject

As compared to younger women, breast deformation when an elderly woman is leaning forwards can be readily observed and is more evident. Hence, a healthy 66 year old woman is selected as the subject in this study. She had a height of 154 cm, a weight of 54.2 kg, and a body mass index of 22.85 kg/m^2. Her bra size was 80 C in the Metric bra sizing system. The project has been approved by the University Human Subjects Ethics Committee. Before the experiment, informed consent has been obtained from the subject.

2.1.2. 3D body scanning

A 3D laser body scanner (Vitus, Human Solutions, Germany) was used to capture a subject's body surface with and without a bra, at a high resolution of 300 pixels/cm^2. As the breast roots of nude ptosis breasts were invisible, the subject was also instructed to wear a single-layer, flexible-wired bra to gently support her breasts with proper tension (Yu, 2016) to ensure a good fit.

2.2. 3D image processing

The raw data of the body point cloud acquired were then imported into Geomagic software (Geomagic Studio 12, USA) to generate the 3D surface of the upper torso. Anatomically, the breast is attached to a bony thorax with subcutaneous tissue around it (Hsu et al., 2011). Therefore, the rigid torso extracted by removing the breasts and a uniform thickness of 2.3 cm of the chest wall soft-tissue (McLean et al., 2011) was used to control for the leaning motion in space. A commercial FEM software, Marc (MSC. Marc 2014.2.0, US), was used to simulate the nonlinear deformation of the breasts under gravity and during forward-leaning. The meshed body model contained 4-node tetrahedral elements which were 20 mm each in length. The constructed model of each part in the FE simulation is shown in Fig. 1.

The 3D scanned image of the bare breast was used to identify the coordinates of the bust points and front neck point. The variation in the breast shape due to wearing a bra was compensated for by applying an external load in the FE model until the bust points had coordinates that

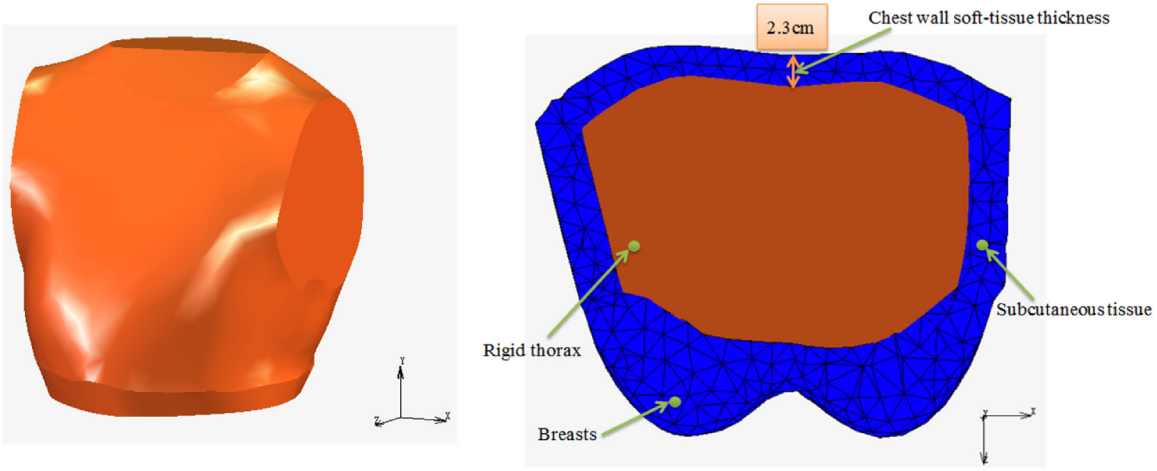

Fig. 1. Rigid torso (a) is extracted by removing breasts and using uniform thickness of 2.3 cm for chest wall (b).

accorded with those of the nude image.

2.3. Material parameters

In this study, the FE body model consisted of a rigid thorax, flexible breasts and a deformable layer of soft tissues. The material property of the layer of subcutaneous tissues has a higher stiffness than the soft breasts. The breasts were assumed to be a homogenous hyper-elastic object with uniform density and consistent material property during postural changes. For hyper-elastic material with nonlinear behavior, the relationship between stress and strain can be derived from a strain energy density function. The strain energy density function describes the energy per unit volume which can be written as Eq. (1).

$$W(I_1, I_2) = \sum_{i,j=0}^{n} C_{ij}(I_1-3)^i(I_2-3)^j \tag{1}$$

where C_{ij} represents the hyperelastic parameters which characterize the nonlinear elastic behavior of the breast material. I_1 and I_2 are the first and the second invariants of the components of the left Cauchy-Green deformation tensor B, which has the forms

$$I_1 = tr(B)$$
$$I_2 = \frac{1}{2}[(tr(B))^2 - tr(B^2)] \tag{2}$$

where $B = F \bullet F^T$, and F is the deformation gradient.

When n is equal to 2, the material is referred to as a Mooney-Rivlin material. In this study, 5 coefficients (C_{10}, C_{01}, C_{11}, C_{20}, and C_{02}) were defined to represent their nonlinear behavior. Initial values for the coefficients in the first trial of FE simulation were based on the *ex-vivo* breast properties measured by Samani and Plewes (Samani and Plewes, 2004). The specific coefficients for the material properties of the breasts and the body are given in Table 1.

2.4. Motion analysis of breast deformation during forward-leaning

In the forward-leaning motion, there is no arm rotation. The breast deformation induced by adopting a forward-leaning angle and the gravity force was used as the boundary condition for the FE model. The dynamic deformation of the breasts against time during the forward-leaning movement was recorded in an experiment using a 12-camera motion capture system (Eagle Motion Analysis Corporation, USA). Two 12.5 mm diameters, spherical retro-reflective markers adhered to the subject's unsupported breasts and 4 markers were attached to the body landmarks (Fig. 2a).

As shown in Fig. 2, using the skeletal items as reference, the straight line connecting the 1st lumbar bone L1 (the middle point between the body markers LPSIS and RPSIS) and the 7th thoracic bone T7 (same location as the Mid-back) was regarded as the back center line, to be used for the sagittal plane (*yoz*) in the FE simulation. In this study, compared to the predominant rotation of the sagittal plane, the relatively small motion in the x-direction was neglected. The leaning angle θ was the intersection angle between the y axis and the body's back center line, calculated using Eqs. (3) and (4).

Table 1
Initial set of coefficients for material parameters used in the FE body model.

Components	Parameters	Value
Soft breast	Density (kg/m^3)	1000
	C_{10} (KPa)	0.3 (Samani and Plewes, 2004)
	C_{01} (KPa)	0.31 (Samani and Plewes, 2004)
	C_{11} (KPa)	2.25 (Samani and Plewes, 2004)
	C_{20} (KPa)	4.72 (Samani and Plewes, 2004)
	C_{02} (KPa)	3.8 (Samani and Plewes, 2004)
Layer of soft tissue	C_{10} (KPa)	5
	C_{01} (KPa)	5

$$y_{L_1} = \frac{y_{LPSIS} + y_{RPSIS}}{2}, z_{L_1} = \frac{z_{LPSIS} + z_{RPSIS}}{2} \tag{3}$$

$$\theta = arctan\frac{z_{T7} - z_{L1}}{y_{T7} - y_{L1}} \tag{4}$$

where the axes x, y and z represented the medial-lateral (+ve left), superior-inferior (+ve up) and anterior-posterior (+ve front) directions respectively.

3. Static and dynamic models to optimize the solution for the material coefficients

In order to find the nonlinear hyperelastic properties of the breasts, iterative changes to the input material coefficients in the FE model were made to simulate the breast deformation during forward-leaning. The optimal values of the material coefficients were determined by minimizing the root mean square error (RMSE) in the difference between the simulated and experimental values. However, the possible range for the material coefficients (C_{01}, C_{10}, C_{11}, C_{02} and C_{20}) was unknown, and hence the search for the optimal solution for the material coefficients involved a process of compressing the initial range reported in previous literature. The dynamic model would have involved time-consuming searching for the optimal solutions and many iteration steps in simulating the forward-leaning results. However, it was simple to use a static FE model to simulate the breast deformation by applying the gravity load to a breast mass at a single posture. Therefore, it was considered to be more practical to first use the static model to determine an initial solution for the range and then use the dynamic model to refine the solution. By combining the static and dynamic models, the optimal solution for the hyperelastic material parameters could be found more efficiently and effectively.

3.1. Static models to compress the range of possible solutions

The static model was constructed under gravity loading in a certain position. By comparing the results with those of the motion capture experiment, the model is expected to find the initial range for the material coefficients of the breasts in a highly efficient way. There were three major steps in finding the optimal range of material parameters by simulating the breast deformation at static postures.

3.1.1. Step 1: Determine the optimal range of material parameters using the static method

In this study, the optimization design method GSSM (Golden Section Search Method) was adopted to gradually compress the initial interval [*a,b*] using the Golden Section Ratio.

Consider an objective function $f(\alpha)$, which is continuous and unimodal over the variable α in the interval [a, b], any two points α_1 and α_2 can divide the interval into three sections. As the Golden Section Ratio is 0.618, $\alpha_1 = b\text{-}0.618(b\text{-}a)$ and $\alpha_2 = a + 0.618(b\text{-}a)$ respectively. There are two possible scenarios for a minimization function.

- If $f(\alpha_1) < f(\alpha_2)$, the minimum should be between a and α_2, the range will become [a, α_2], so we rename α_2 as b and rename α_1 as α_2.
- If $f(\alpha_1) \geq f(\alpha_2)$, the minimum should be between α_1 and b, the range will become [α_1, b], so we rename α_1 as a and rename α_2 as α_1.

After the interval becomes smaller, it will be divided again into 3 sections for the repeating steps to compress the new interval. Once a particular iteration can satisfy the termination criterion $|a\text{-}b| < \varepsilon$, the optimum interval is determined (Rao, 2009). By iteratively adjusting the material variable α, the objective function is evaluated, in order to gradually compress the interval of possible solutions for the material coefficients to ultimately derive the optimal solution.

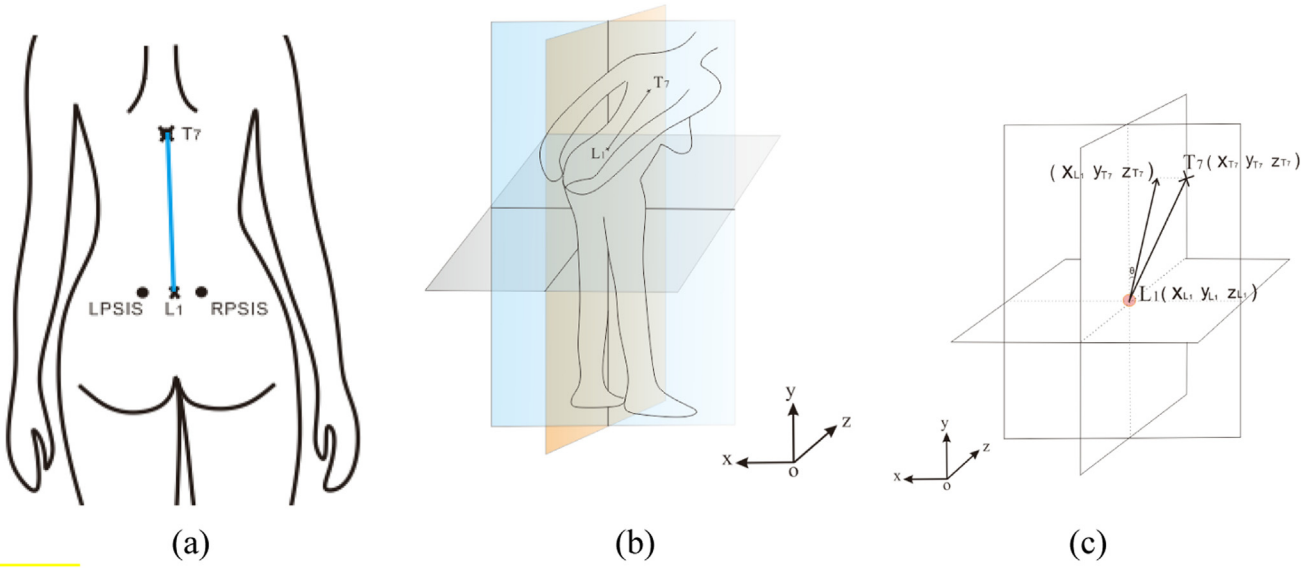

Fig. 2. The skeletal items, 1st lumbar bone L1 and the 7th thoracic bone T7, are marked in the motion capture system (Eagle Motion Analysis Corporation, USA) to define the back center line (a). The back center line of the body in space is shown in (b) and the leaning angle θ (c) is the intersecting angle between the y axis and the back center line.

3.1.2. Step 2: Define the objective function

In this study, the objective function was to minimize the difference between the FE simulation result based on a 3D geometric model and the motion capture experimental data. The result was expressed in terms of the nipple distance (i.e. the straight distance between two nipple points). This distance effectively represents the large deformation in the breasts in a static posture at a forward-leaning angle of 45°. The incremental change in nipple distance ΔL is defined as the criterion, shown in Eq. (5),

$$\Delta L = \frac{L_e - L_0}{L_0} \text{x} 100\% \tag{5}$$

where L_0 is the nipple distance at the initial upright standing position. L_e is the nipple distance at the end position where the leaning angle is 45°.

When searching for the optimal solution for the material coefficients, a compensation factor α applied to the initial set of material coefficients was systematically iteratively changed (Table 1) using the GSSM. The new iterative material coefficients were obtained by dividing the initial ones by the compensation factor α. The Relative Error (RE) was used as the objective function $f(\alpha)$ and is presented in Eq. (6),

$$f(\alpha) = \frac{(\Delta L_{Exp} - \Delta L_{FEM})}{\Delta L_{Exp}} \tag{6}$$

where ΔL_{Exp} denotes ΔL calculated in the experiment and ΔL_{FEM} denotes ΔL predicted by the FE simulation. In this static method, the ΔL at only two body postures (standing upright at the initial condition and leaning at 45°at the end position) were measured.

3.1.3. Step 3: Simulate the breast deformation at a static position

The unloaded geometry of the FE body model in a gravity-free state needed to be prepared by applying an upward load to counteract the gravity force. The configuration of the breast before deformation was saved as the initial geometry prepared for the FE simulation. The FE model contained only the geometry with the FE mesh and the material coefficients but there was no internal stress. Then, the body model was tilted to the initial condition and the end position respectively (Fig. 3), with gravity loading applied to the breasts. The breasts and subcutaneous tissues were attached to the rigid torso by using a glued interaction found in the software as a type of contact in the model. There was no sliding between the flexible soft tissues and rigid torso. When upward gravity or a gravity load was applied, the rigid torso was fixed so the nodes of the surface of the inside of the soft tissues which were attached to the rigid torso were also fixed. Then the simulated ΔL was compared with that of the experimental results. This process was repeated until the minimum value for f(α) was found. The workflow for this method is shown in Fig. 4.

In order to examine the sensitivity of the model to mesh refinement, a mesh convergence study was conducted to determine the influence of the mesh density. Three mesh densities were considered: coarse (average element size of 30 mm), medium (average element size of 20 mm) and fine (average element size of 10 mm). It was observed that by increasing the number of mesh elements, there is a 2% variation in the nipple distance in the static position between the results of the coarse and medium meshes, and 0.8% between the medium and fine meshes. However, the calculation time required for the fine mesh condition is 5 times more than that for the medium mesh condition. Therefore, the medium mesh is used in both the static and dynamic simulations to ensure the accuracy of the predicted results and reduce the CPU time.

3.2. Dynamic model to refine the optimal material parameters

After finding the optimal range for the material coefficients using the static method, the dynamic method was used to refine the static optimal solution. The workflow for the method for the dynamic FEM simulation of the angle-dependent breast deformation during forward-leaning is shown in Fig. 5.

To determine the optimum solution for the material parameters, the compensation factor α is changed iteratively by using a fixed step length Δα to refine the interval from a to b as shown in Eq. (7) until the simulation result is as close as possible to that of the experimental data, i.e. the relative RMSE is minimized.

$$\alpha_i = a + i\Delta\alpha \quad \left(where i = 1, 2, .., \frac{|b-a|}{\Delta\alpha}\right) \tag{7}$$

There were three major steps in refining the optimal material parameters by simulating the breast deformation in the dynamic forward-leaning process.

Step 1. Input the breast parameters into the FE model and apply the

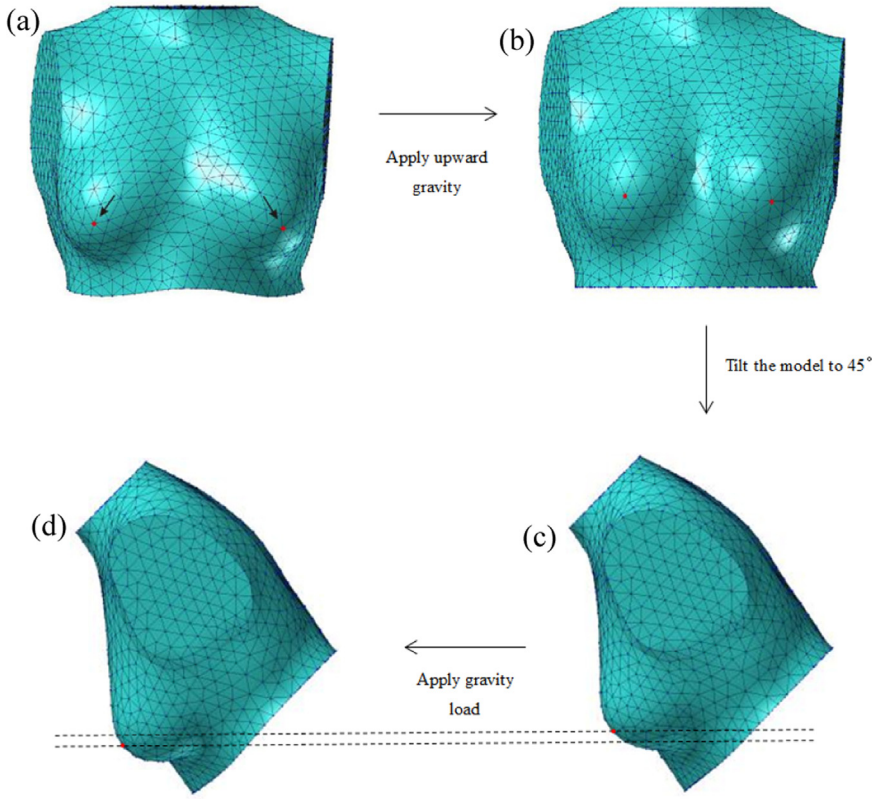

Fig. 3. Simulation process for static forward-leaning posture starts from applying upward gravity to the nude breast model (a) to obtain the gravity-free state (b) as the initial configuration for FE simulation. (c) Then the model is tilted to end position of 45°, (d) followed by applying gravity to breasts.

upward gravity load to obtain the gravity-free FE model.

Step 2. Apply the boundary condition to the model with gravity load and rotation.

Step 3. Find the minimum RMSE result for different sets of material coefficients.

3.2.1. Theoretical formulae for the forward-leaning problem in finite element analysis

The process of the forward-leaning motion can be regarded as a coupled system (Hu et al., 2002) of a rigid thorax and flexible breasts. When the torso leans forward, the rigid body rotates around the X-axis in the Global Coordinate System (GCS), while the flexible breasts deform due to the gravity load with reference to a Local Coordinate System (LCS) (Fig. 6). In order to simplify the formulation of the finite element system, the LCS shared the same original point with the global coordinate.

The point M represents any point on the deformable breast expressed in a vector form $\boldsymbol{R}$ in the Global Coordinate System. The point M_0 is the pre-deformed state of the point M.

$$\{\boldsymbol{R}\} = [\mathrm{A}](\{\boldsymbol{r_0}\}+\{\boldsymbol{r_f}\}) \tag{8}$$

where $\boldsymbol{r_0}$ is the position vector without deformation and $\boldsymbol{r_f}$ is the position vector with deformation in the Local Coordinate System. [A] is a matrix for the local coordinates to be transformed to the global coordinates.

$$[\mathrm{A}] = \begin{bmatrix} 1 & 0 & 0 \\ 0 & \cos\theta & \sin\theta \\ 0 & -\sin\theta & \cos\theta \end{bmatrix} \tag{9}$$

The point variables can be expressed by the nodal variables according to the finite element theory (Dhatt, 2012),

$$\{\boldsymbol{r_0}\} = [\mathrm{N}]\{\boldsymbol{u_0}\} \text{and } \{\boldsymbol{r_f}\} = [\mathrm{N}]\{\boldsymbol{u_f}\} \tag{10}$$

where [N] is the matrix of interpolation functions, $\boldsymbol{u_0}$ is the nodal displacement without deformation and $\boldsymbol{u_f}$ is the nodal displacement with deformation in the LCS. The displacement vector of the arbitrary point $\{\boldsymbol{u}\}$ contains a rigid-body (torso) rotation and a flexible body (breast) deformation.

$$\{\boldsymbol{u}\} = \{\boldsymbol{u_0}\}+\{\boldsymbol{u_f}\} \tag{11}$$

Substituting Eqs. (10) and (11) into Eq. (8), the displacement vector of the points in the GCS can be written as

$$\{\boldsymbol{R}\} = [\mathrm{A}][\mathrm{N}]\{\mathrm{u}\} \tag{12}$$

The velocity vector is the first order derivative of the position vector

$$\{\dot{\boldsymbol{R}}\} = [\mathrm{A}_\theta][\mathrm{N}]\{\boldsymbol{u}\}\dot{\theta} + [\mathrm{A}][\mathrm{N}]\{\dot{\boldsymbol{u}}_\boldsymbol{f}\} \tag{13}$$

where $[A_\theta]$ is the first order derivative of [A] respect to the rotation angle θ.

The kinetic energy can be written as,

$$\mathrm{E}_k = \frac{1}{2}\int^{V} \rho\{\dot{\boldsymbol{R}}\}^T\{\dot{\boldsymbol{R}}\}\mathrm{d}V \tag{14}$$

ρ is the density of the breast, and V is the volume of the breast. $\{\dot{\boldsymbol{R}}\}^T$ is the transposed matrix of $\{\dot{\boldsymbol{R}}\}$.

In the forward-leaning rigid-flexible coupled system, the rotation angle $\theta$is obtained from the motion analysis (Section 2.4) which can then be inputted into the FE software as the boundary condition (Section 3.2.2). The only unknown variable is the displacement of every material point in the flexible breasts due to their deformation $\{u_f\}$ under gravity.

Using the Lagrange's equation, the dynamic equation of the coupled system can be expressed as

$$\{M_{\theta f}\}\ddot{\theta} + \{M\}\{\ddot{\boldsymbol{u}}_\boldsymbol{f}\} + [C]\{\dot{\boldsymbol{u}}_\boldsymbol{f}\} + [K]\{\boldsymbol{u_f}\} = \{Q\} \tag{15}$$

where $\{M\}$ is the mass matrix. $[C]$ and $[K]$ are the matrix of the damping

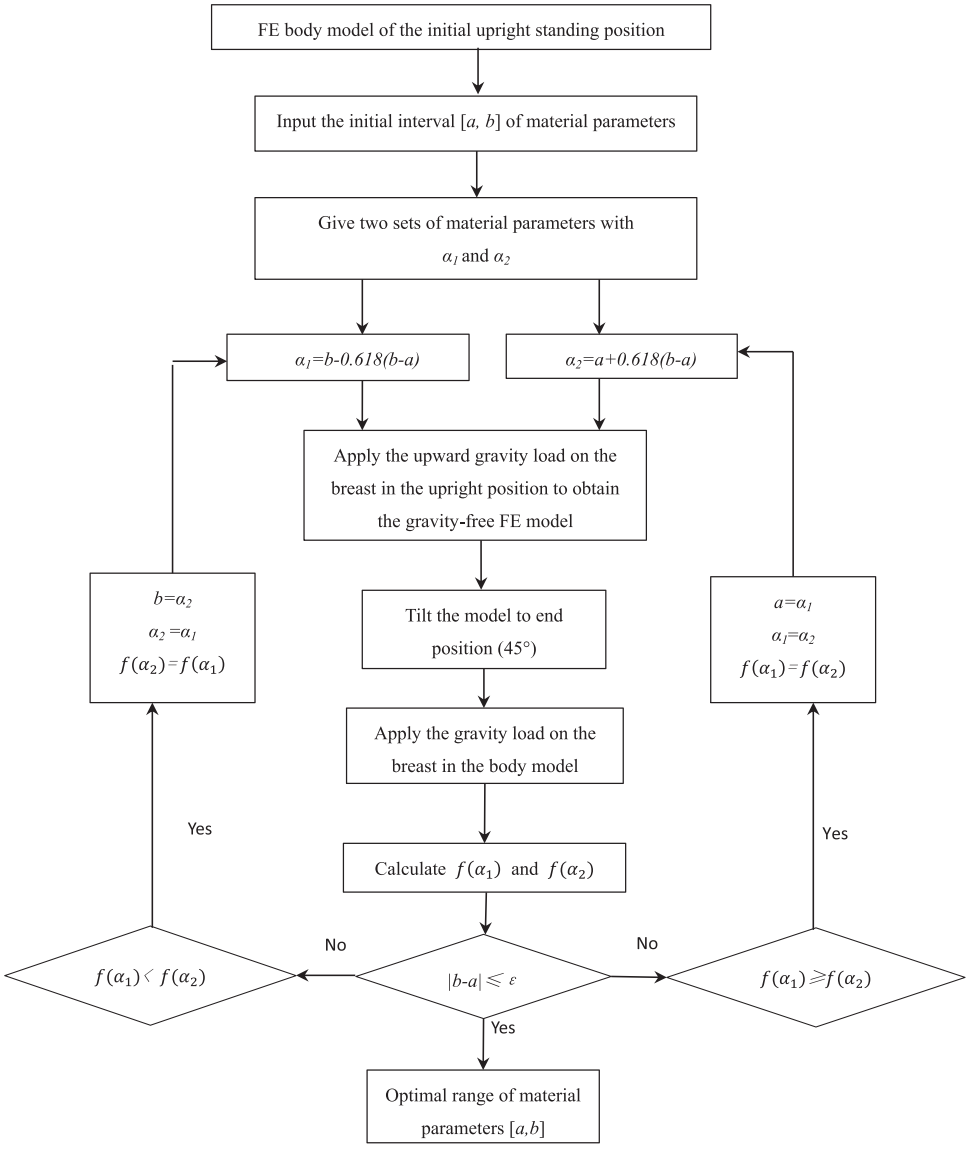

Fig. 4. Workflow for the static model to find the optimal material coefficients range.

ratio and stiffness respectively. $\{M_{\theta f}\}$ representing a row vector of this coupled components at the element level has a form

$$\{M_{\theta f}{}^e\} = \{\boldsymbol{u}\}^T[H^e] \tag{16}$$

where

$$[H^e] = \int_{V^e} \rho[N]^T[A_\theta]^T[A][N]dV$$

Eq. (15) presents the external load $\{Q^e\}$ applied to the element which contains gravity $\{G^e\}$, centrifugal $\{F_{ce}{}^e\}$ and Coriolis forces $\{F_{co}{}^e\}$ (Hu et al., 2002).

$$\{Q^e\} = [N]T\{G^e\} + \{F_{ce}{}^e\} + \{F_{co}{}^e\} \tag{17}$$

where

$$\{F_{ce}{}^e\} = \rho\dot{\theta}^2([P_1]\{u\} - [P_2]\{u_f\})$$

$$\{F_{co}{}^e\} = 2[H^e]\{\dot{u_f}\}\dot{\theta}$$

$$[P_1] = \int_{V^e} [N]^T[A_\theta]^T[A_\theta][N]dV$$

$$[P_2] = \frac{1}{2}\int_{V^e}(L^2 - y^2)\frac{\partial\{S_1\}^T}{\partial y}\frac{\partial\{S_1\}}{\partial y}dV + \frac{1}{2}\int_{V^e}\left(L^2 - y^2\right)\frac{\partial\{S_3\}^T}{\partial y}\frac{\partial\{S_3\}}{\partial y}dV$$

where L is the cross-sectional level of the leaning body model in FEM, $\{S_1\}$ and $\{S_3\}$ are the row vectors in the interpolation function [N].

3.2.2. Boundary condition for the FE simulation

In the FE simulation of the forward-leaning motion with respect to the Global Coordinate System, the rotation center was the 1st lumbar bone (L1) in accordance with the experiment as shown in Fig. 2(a). The upper body was rotated along the line that passes through the rotation center L1 and parallel to the x-axis. The rotation line was fixed during forward-leaning. The boundary condition for the forward-leaning motion to be entered into the FE simulation was derived from the rotation angle of the center back line of the body plotted against time obtained from the motion capture experiment. The motion camera captured the real-time displacement of each marker. However, the data inevitably contained noise affected by the surroundings. To avoid the disturbance of the processed data being amplified during the FE simulation, the data noise was filtered using the concept of the moving average, in order to smooth out abnormal fluctuations and to remove the outliers for the time-dependent data. This filter averages M input points and produces a single output point $y[i]$, written by

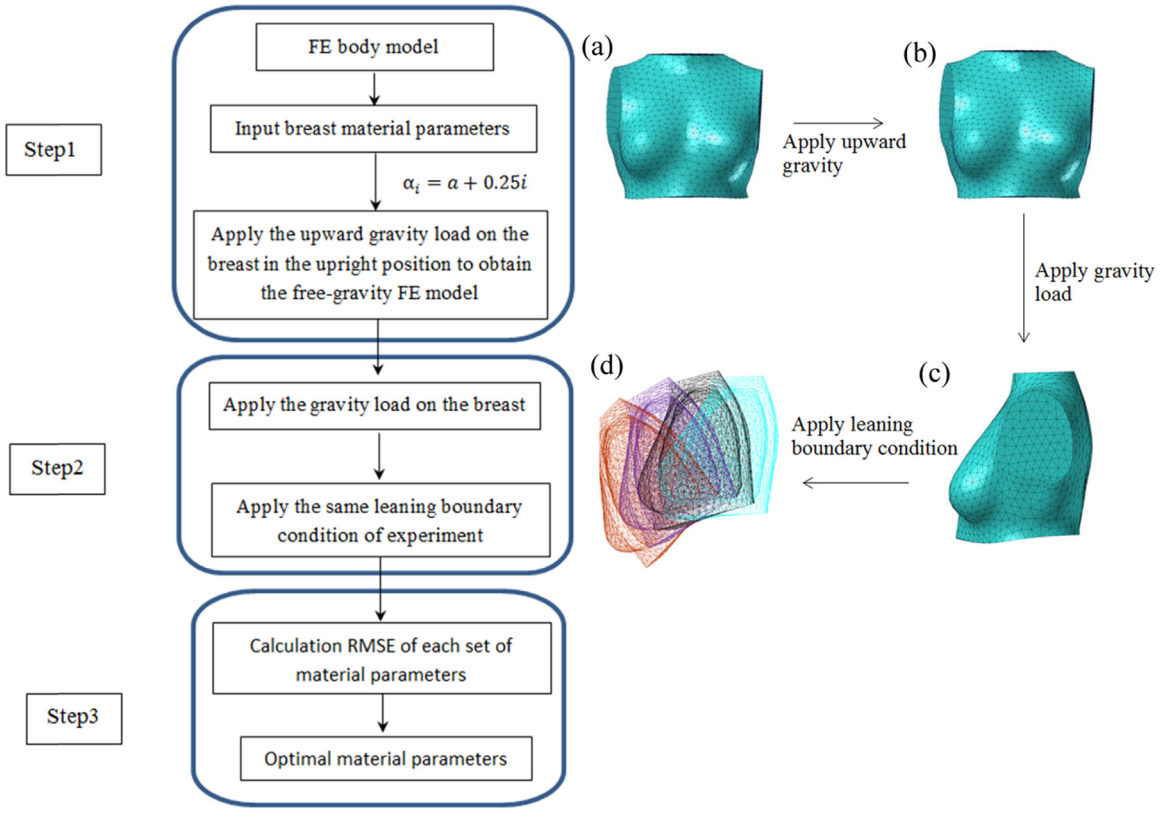

Fig. 5. The simulation process for the dynamic model starts from applying upward gravity to the nude breast model (a) to obtain the gravity-free state (b) as the initial configuration for FE simulation. (c) Then boundary conditions of gravity loading and (d) rotation are applied to model. The calculated RMSE of each material parameter is compared with that of experiment to find optimal solution.

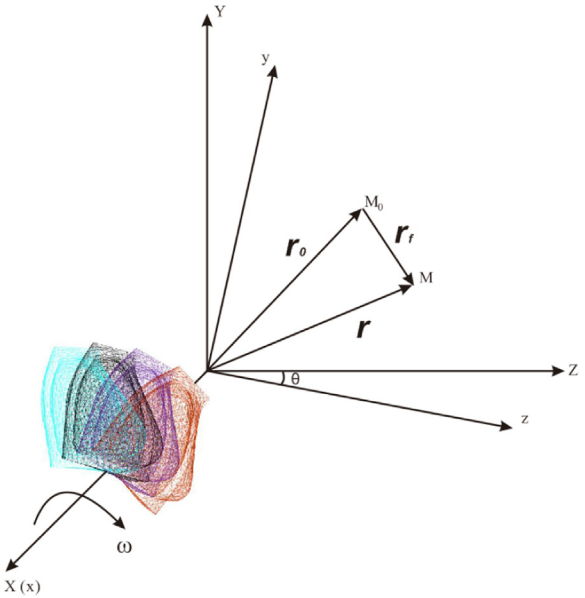

Fig. 6. Global and local coordinates of the rigid-flexible coupling system.

$$y[i] = \frac{1}{M}\sum_{j=0}^{M-1} x[i+j] \tag{18}$$

where $x[i]$ is the input signal, $y[i]$ is the output signal, M is the number of points used in the moving average calculation (Steven et al., 2002). The data processing was conducted using the mathematical software Matlab (R2015b, MathWorks, USA). In order to avoid excessive filtering or ineffective smoothing of the program, the value of M in the equation was pre-set to be 5 after repeated trials were carried out. The angular acceleration, which is derived by differentiating the rotation angle twice with respect to time, exhibited drastic fluctuations and therefore required filtering. The fluctuation of the filtered acceleration was only around 1/400 of the original one, so the filtered angle-time curve was applied to the FE model as the boundary condition for simulating the dynamic breast deformation during forward-leaning. It was confirmed that the results of the incremental change in nipple distance with filtering for the boundary condition are clearer than those without.

3.3. Validation method

In the dynamic model, the nipple distance changed with time. The accuracy of the FE simulated result was evaluated based on the average value of the RMSE across all of the sample data points of the leaning angle given by

$$RMSE = \frac{1}{n}\sqrt{\sum_{i=1}^{n}\left(\frac{\Delta L_{Exp,i} - \Delta L_{FEM,i}}{\Delta L_{Exp,i}}\right)^2} \tag{19}$$

where ΔL_{Exp} denotes the incremental change in nipple distance in the experiment, ΔL_{FEM} denotes the incremental change in nipple distance predicted by the FEM, n is the number of points independently and uniformly distributed in the interval from the leaning angle in the initial upstanding position (1.87°) to the end position (45°). In this research study, a total of 432 sample points is obtained by setting the step length to 0.1°. The smaller that the RMSE value is, the more accurate is the set of the material parameters that has been inputted into the simulation. The objective was to determine those material parameters that generated the minimum RMSE.

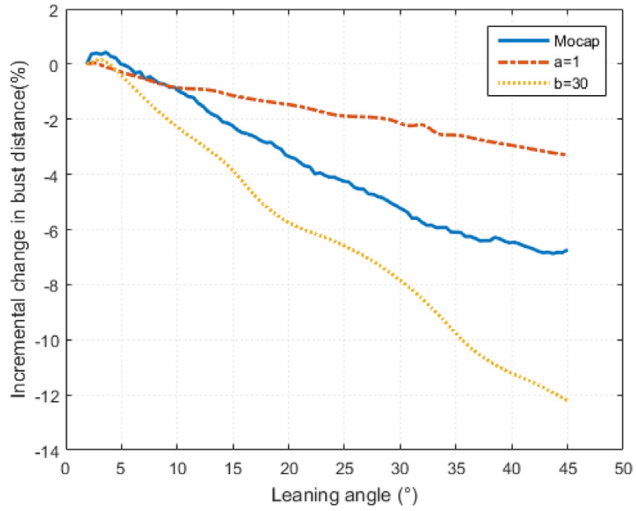

Fig. 7. Comparison of predicted and experimental incremental change in nipple distance v leaning angle for an initial range of α values.

4. Results and discussion

4.1. Optimal solution for the material parameters for the breasts

In this study, the optimal solution to determine the material parameters of the breast tissues was investigated. Following the workflow of the GSSM (Fig. 4), two compensation factors were used for the initial set of material coefficients (Table 1). Fig. 7 shows that the optimal value for α should have been between 1 and 30, in order to minimize the RMSE and give the best match with the motion capture experimental data.

The range for the optimal solution to be derived from the static model was first defined within the initial interval [a, b] = [1, 30]. Several iterations of the GSSM were performed using values of α_1 and α_2 (Table 2) until the termination criterion $\varepsilon = |b\text{-}a| \leq 2$ was satisfied. After six iterative steps of the GSSM, the interval for α [6.229, 7.844] was found to be optimum with a value for $\varepsilon = 1.615$.

To determine a more accurate optimal solution for the material parameters, the dynamic model was used. Based on the rough optimization using the static model, the search range for the compensation factors α was set to be [6, 8] for further iteration within this range, and iterations were performed using a smaller iterative step change of 0.25 for the value of α. As shown in Table 3, nine compensation factors denoting nine different sets of material coefficients (C_{10}, C_{01}, C_{11}, C_{20}, and C_{02}) were tried in the dynamic models (M1-M9) to simulate the breast deformation in terms of the incremental change in nipple distance. The minimum relative RMSE between the simulated ΔL_{FEM} and experimental ΔL_{EXP} was then determined as shown in Table 3.

Table 3 shows that the compensation factor α = 7.25 gave the minimum relative RMSE of 0.33%. As shown in Fig. 8, the dynamic incremental change in nipple distance in the material model M6 matched the experimental data overall better than that in the M1 model

Table 2
The iterative steps to derive the optimal range using the GSSM.

Iterative step	a	b	α_1	α_2	$\lvert b\text{-}a\rvert$
1	1.00	30.00	12.08	18.92	29.0
2	1.00	18.92	7.85	12.08	17.9
3	1.00	12.08	5.23	7.85	11.1
4	1.00	7.85	3.62	5.23	6.8
5	3.62	7.85	5.23	6.23	4.2
6	5.23	7.84	6.23	6.85	2.6
7	6.23	7.84	–	–	1.6

Table 3
RMSE of different material types.

Material model	M1	M2	M3	M4	M5	M6	M7	M8	M9
Compensation factor α	6.00	6.25	6.50	6.75	7.00	**7.25**	7.50	7.75	8.00
RMSE(%)	7.25	5.78	4.35	2.97	1.63	**0.33**	0.96	2.19	3.41

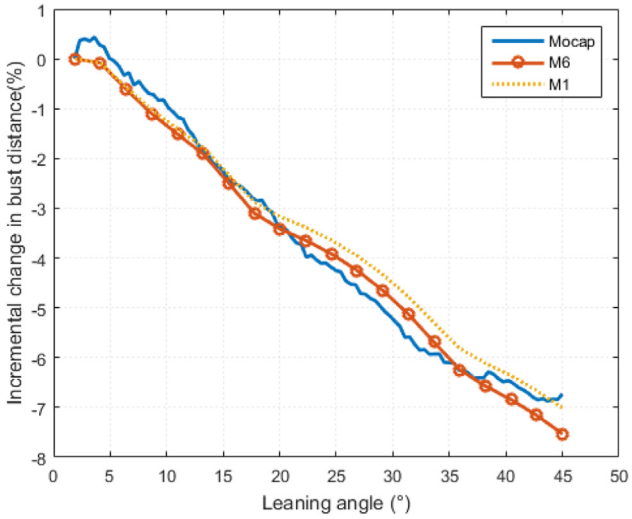

Fig. 8. Comparison of the predicted incremental change in nipple distance for the M1 and M6 material models with the experimental data.

during the leaning process especially in the section before a leaning angle of 38° was reached. It, therefore, confirmed that the dynamic FE model could successfully find the optimized solution for the compensation factor for a set of material parameters with a relative RMSE < 0.5%.

It is also noted that the incremental change in nipple distance increased as an absolute percentage with an increase in leaning angle. This implied that the two nipples continuously converged towards each other during the process of forward-leaning.

4.2. Breast deformation during forward-leaning simulated with the optimal material parameters

Using the optimal material model M6, the 3D breast deformation at the initial upright standing position and different leaning angles of 15°, 30°,45° was simulated and presented in terms of horizontal x-displacement that can visually show the detailed mechanism of the breast deformation during forward-leaning. The simulation results were also verified with motion capture experiment (Fig. 9).

Fig. 9a shows that gravity loading causes the breasts to deform laterally which means that the breasts are moving “east and west”. From the results of the FE simulation of breast deformation during forward-leaning, the interesting findings include:

- The gravity has caused an inward and downward breast displacement towards the center front of the body. This phenomenon becomes more obvious when the leaning angle increases. Larger displacement of the sides and bottom of the breasts is evident converging them even more towards the center front, whilst the upper breasts are spread less sideways.
- This trend of breast convergence during forward-leaning becomes saturated at a leaning angle of 45° (Fig. 9d). The largest displacement occurs in the nipple region and gradually decreases for the areas around it. There is almost no displacement of the medial parts and the top parts of the breasts.

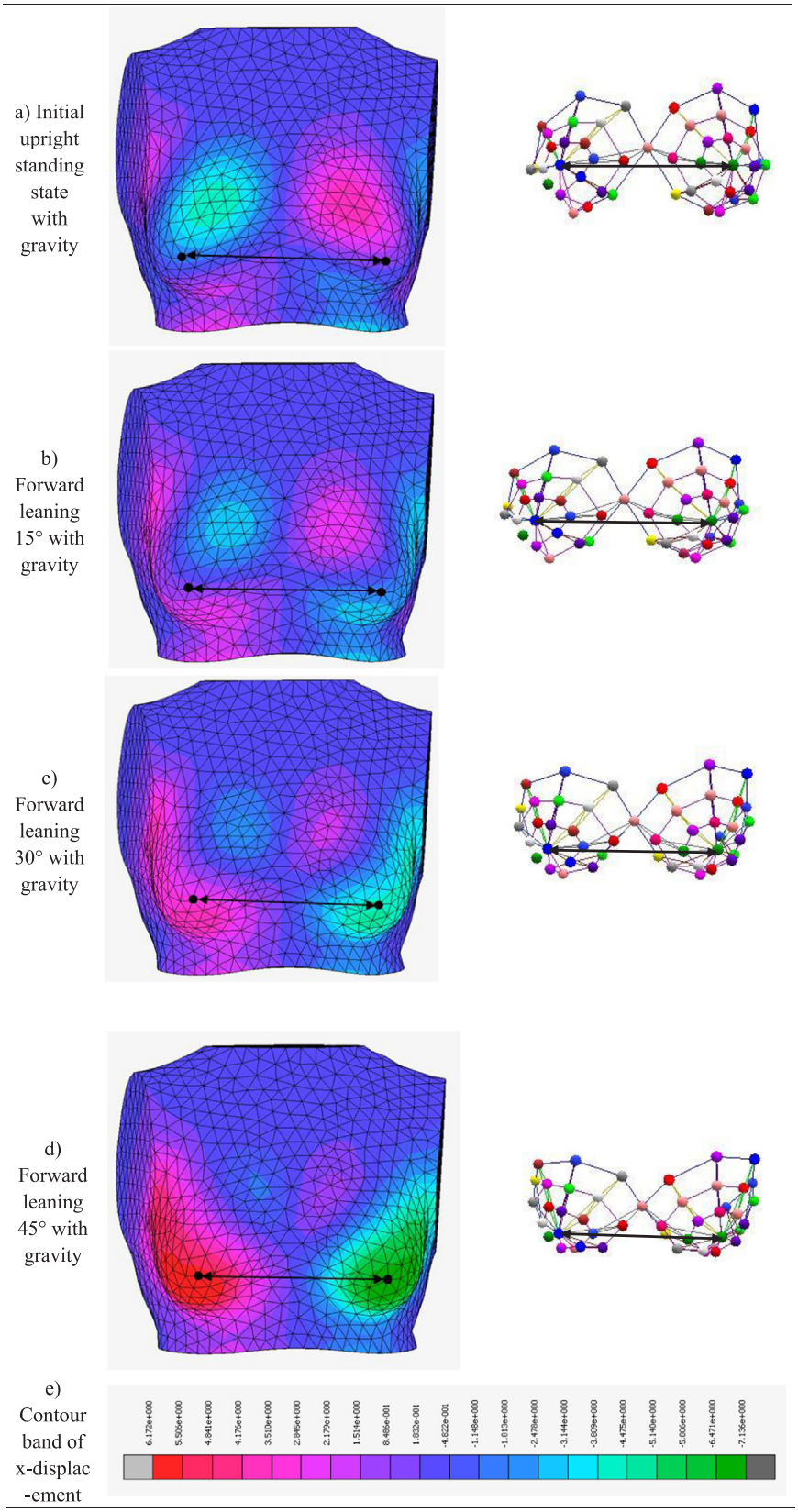

Fig. 9. Dynamic simulation of x-displacement of the breast by using the optimal material model (length of the double-headed arrow is the bust distance, i.e. distance between two nipples) and comparison with the motion capture images.

The breast shape in Fig. 9d is similar to the nice shape provided by adequate bra support, which prevents the two breasts "going east and west". The color profile of the x-displacements also validates with the fact that a supportive bra should uplift the breasts from the side and bottom areas towards the center front, in order to achieve the target that the lateral forces are all compensated by the bra force. This FE simulation model, using realistic nonlinear material parameters for the breasts, has successfully demonstrated realistic breast deformation. This finding can also explain the mechanism of how the breasts can be shaped nicely by external forces using bras.

4.3. Prediction of breast displacement during walking using the optimal material parameters

With the optimal sets of material parameters, the validated FE model can be used to predict the deformation of the breast during other daily activities such as running, stepping or walking. In this research, additional motion capture experiment on the same subject was conducted to capture the deformation of the breasts during walking. The displacement of the right nipple point was selected as the representative marker to compare the results of simulation and experiment. The subject was required to walk on a treadmill at the speed of 2.5 km/h. The displacements of the clavicle in three directions (x, y and z) were extracted from the motion capture data and input into the FE model as the boundary condition to control the movement of the torso. It is noteworthy that the breast displacement in z-direction was neglected in this study since it was much relied on the arms that moved back and forth during walking. Therefore, the current FE model without muscle and skin could not fully simulate the displacement in z-direction. Figs. 10a and 10b compare the actual displacement (x and y-direction) of right nipple point in the experiment and the predicted displacement based on the FE model using the optimal material model M6.

Table 4
RMSE of the simulated right nipple point displacement in x and y directions.

Displacement direction	x	y
RMSE(%)	0.12	0.06

The results show that the clavicle displacement representing the movement of the rigid torso has a smaller amplitude. The displacement of the soft breast contains two components, i.e. the rigid movement of the torso and the flexible deformation of soft tissues. The vibration curve obtained from the simulation are aligned with the experimental curve. Table 4 shows that the FE model with optimal material type M6 can effectively predict the breast displacement within a reasonable

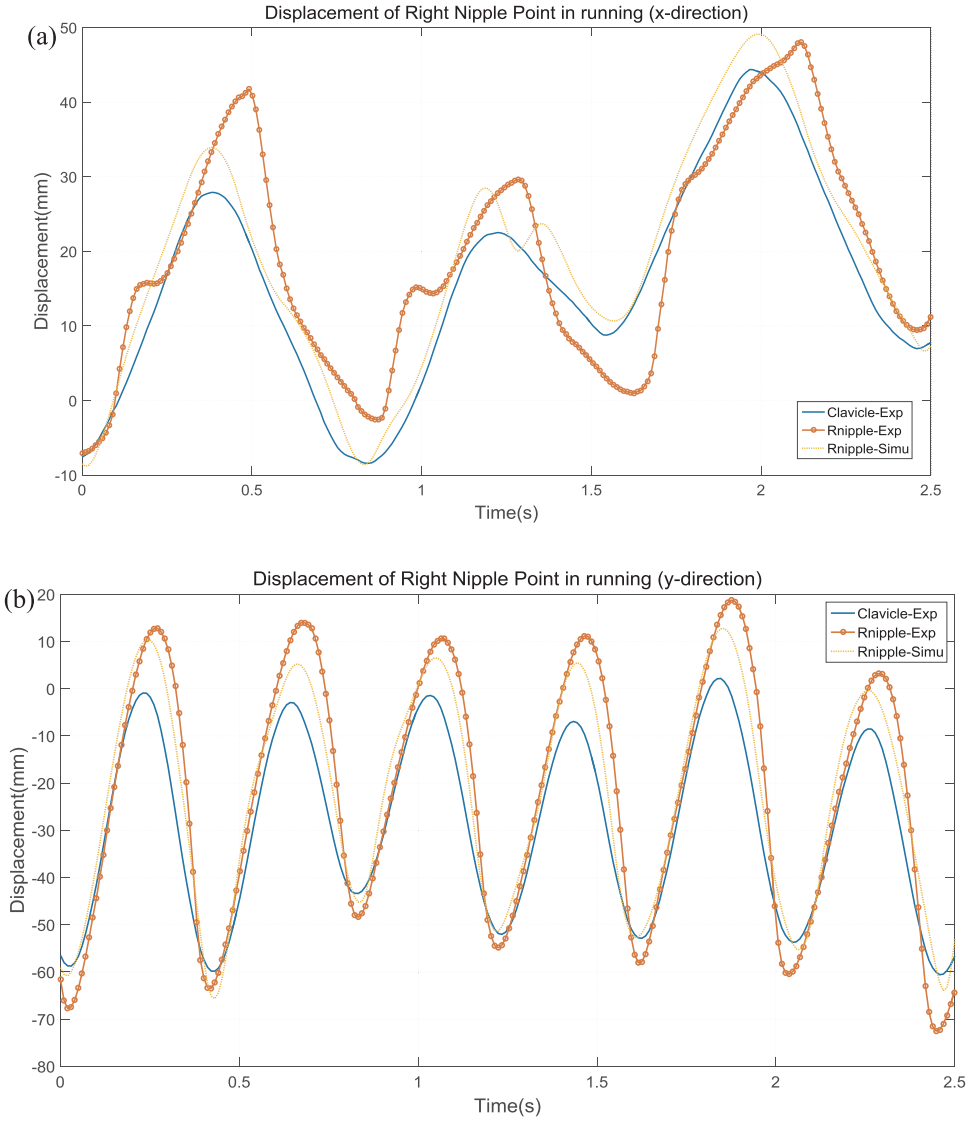

Fig. 10. Experimental and simulated displacement of the right nipple point in the x and y direction.

RMSE error.

This preliminary study has some primary limitations. The breast was regarded as a uniform structure with one type of material property. The geometrical configuration was not constructed with different proportions of fatty and fibro-glandular tissues which have different material properties. It is acknowledged that there was only one subject being analyzed in this study. Further studies are recommended to build the FE models based on more subjects to observe the stabilities of the method. It should also examine the dynamic change of biomechanical model of breast involving different components with various material properties. Nevertheless, the study provides preliminary evidence that it is possible to obtain the non-linear material parameters of breasts by using static and dynamic FE models in-vivo. The predicted material parameters of the breasts can also provide the basis for future studies to investigate the contact mechanism between breasts and garments. The contact mechanism shows the breast deformation in a bra and the pressure distribution in the contact area. Future research should consider a wider age range of subjects to evaluate the accuracy of the static and dynamic FE models and include more complicated structures for the breast model.

5. Conclusion

The primary contribution of this study is a new optimization method that combines static and dynamic FEMs to generate nonlinear Mooney-Rivlin material coefficients for the breasts in-vivo and validate the simulated results of breast deformation in the forward-leaning position with data from motion capture experiments. In order to search more efficiently for the optimal solution to find the parameters, the static model is initially used to calculate the “incremental changes in nipple distance” by systematically iterating the model with different sets of hyperplastic breast material coefficients based on the Golden Section Search Method. The dynamic model is then used to fine-tune the optimal range of the compensation factors derived from the iterative solutions to the static model. In the FEM of simulating dynamic motion, the process of forward-leaning is formulated as a coupled system that comprises a rigid thorax and two flexible breasts. The dynamic equation of the breast deformation during forward-leaning is developed with gravitational loading and centrifugal and Coriolis forces. The boundary conditions are the filtered forward-leaning angle vs time curve obtained from the motion capture experiment. The material coefficients of the breast tissues are modified by using compensation factor α iteratively until the overall RMSE between the predicted and experimental data for the rate of change in nipple distance is minimized. By combining the static and dynamic FE models, the optimal solution for the nonlinear material coefficient of the breasts is found by obtaining the minimum RMSE (0.33%) between the simulation and experimental data in terms of the rate of change in nipple distance. The breast material coefficient results indicate that the previous measurements of the ex-vivo breast material properties are too high (which causes overly stiff breasts) to accurately simulate the deformation of the breasts in-vivo. The model has proven to be a useful tool to optimize the solution for the material coefficients of breasts with high precision. The new set of Mooney-Rivlin material coefficients can successfully simulate breast deformation when an individual is leaning forward and walking positions with good accuracy. The result provides the scientific basis for future mechanical modeling of breasts in dynamic situations which involve irregular geometrical shapes, nonlinear materials (incompressible Mooney-Rivlin) and large deformations.

Acknowledgement

We thank the financial support from the Research Grants Council, Hong Kong Grant of the project (ref: PolyU 152205/14E), the Central Research Grant, Hong Kong of the project (ref: PolyU 152115/15E) and the Innovation and Technology Fund, Hong Kong ITS/255/15. We also thank the subject who participated in this study, and Dr. Simon Harlock for his professional comments.

References

Cai, Y.Q., Chen, L., Yu, W., Zhou, J., Wan, F., Suh, M., Chow, D.H.K., 2018. A piecewise mass-spring-damper model of the human breast. J. Biomech. 67, 137–143. https://doi.org/10.1016/j.jbiomech.2017.11.027.

Chen, L.H., Ng, S.P., Yu, W., Zhou, J., Wan, K.W., 2013. A study of breast motion using non-linear dynamic FE analysis. Ergonomics 56, 868–878. https://doi.org/10.1080/00140139.2013.777798.

Del Palomar, A.P., Calvo, B., Herrero, J., López, J., Doblaré, M., 2008. A finite element model to accurately predict real deformations of the breast. Med. Eng. Phys. 30, 1089–1097.

Dhatt, G., 2012. Finite element method. London: ISTE; Hoboken, N.J: Wiley, London: Hoboken, pp. 28-33.

Dufaye, G., 2013. Advanced finite element modelling for the prediction of 3D breast deformation. Rev. Eur. De. mécanique Numér. 22, 170–182.

Eder, M., Raith, S., Jalali, J., Volf, A., Settles, M., Machens, H.G., Kovacs, L., 2014. Comparison of different material models to simulate 3-D breast deformations using finite element analysis. Ann. Biomed. Eng. 42, 843–857.

Han, L., Noble, J.A., Burcher, M., 2003. A novel ultrasound indentation system for measuring biomechanical properties of in vivo soft tissue. Ultrasound Med. Biol. 29, 813–823.

Hsu, C.M., Palmeri, M.L., Segars, W.P., Veress, A.I., Dobbins, J.T., 2011. An analysis of the mechanical parameters used for finite element compression of a high-resolution 3D breast phantom. Med. Phys. 38, 5756–5770. https://doi.org/10.1118/1.3637500.

Hu, K., Vlahopoulos, N., Mourelatos, Z.P., 2002. A finite element Formulation for Coupling rigid and Flexible body dynamics of rotating beams. J. Sound Vib. 253, 603–630. https://doi.org/10.1006/jsvi.2001.4066.

Krouskop, T.A., 1998. Elastic moduli of breast and prostate tissues under compression. Ultrason. Imaging 20, 260–274.

McLean, A.R., McLean, A.R., Richards, M., Crandall, C., Marinaro, J., 2011. Ultrasound determination of chest wall thickness: implications for needle thoracostomy. Am. J. Emerg. Med. 29, 1173–1177.

Omidi, E., Fuetterer, L., Reza Mousavi, S., Armstrong, R.C., Flynn, L.E., Samani, A., 2014. Characterization and assessment of hyperelastic and elastic properties of decellularized human adipose tissues. J. Biomech. 47, 3657–3663. https://doi.org/10.1016/j.jbiomech.2014.09.035.

Poplack, S.P., Paulsen, K.D., Hartov, A., Meaney, P.M., Pogue, B.W., Tosteson, T.D., Grove, M.R., Soho, S.K., Wells, W.A., 2004. Electromagnetic breast imaging: average tissue property values in women with negative clinical findings. Radiology 231, 571–580.

Rajagopal, V., Lee, A., Chung, J.-H., Warren, R., Highnam, R., Nash, M., 2008. Creating individual-specific biomechanical models of the breast for medical image analysis. Acad. Radiol. 15, 1425–1436.

Ramião, N.G., Martins, P., Rynkevic, R., Fernandes, A., Barroso, M., Santos, D., 2016. Biomechanical properties of breast tissue, a state-of-the-art review. Biomech. Model. Mechanobiol. 15, 1307–1323.

Rao, S.S., 2009. Engineering Optimization: Theory and Practice. John Wiley& Sons, Inc., Hoboken, New Jersey, pp. 267–271.

Samani, A., Bishop, J., Luginbuhl, C., Plewes, D., 2003. Measuring the elastic modulus ofex vivosmall tissue samples. Phys. Med. Biol. 48, 2183–2198.

Samani, A., Plewes, D., 2004. A method to measure the hyperelastic parameters ofex vivobreast tissue samples. Phys. Med. Biol. 49, 4395–4405.

Schnabel, J.A., Tanner, C., Castellano-Smith, A.D., Degenhard, A., Leach, M.O., Hose, D.R., Hill, D.L., Hawkes, D.J., 2003. Validation of nonrigid image registration using finite-element methods: application to breast MR images. IEEE Trans. Med. Imaging 22, 238–247. https://doi.org/10.1109/TMI.2002.808367.

Skovoroda, A., 1994. Theoretical analysis and verification of ultrasound displacement and strain imaging. IEEE Trans. Ultrason., Ferroelectr. Freq. Control 41, 302.

Steven, S., Smith, S., 2002. Digital Signal Processing: a Practical Guide for Engineers and Scientists. California Technical Publishing, San Diego, California, pp. 277–284.

Sutradhar, A., Miller, M.J., 2013. In vivo measurement of breast skin elasticity and breast skin thickness. Skin. Res. Technol. 19, e191–e199.

Tanner, C., Schnabel, J., Hawkes, D.J., Hawkes, D., Leach, M., Hose, D.R., 2006. Factors influencing the accuracy of biomechanical breast models. Med. Phys. 33, 1758–1769.

Yu, W., 2016. Advances in Women's Intimate Apparel Technology. Woodhead Publishing, pp. 109–133.

Zain-Ul-Abdein, M., Morestin, F., Bouten, L., Cornolo, J., 2013. Numerical simulation of breast deformation under static conditions. Comput. Methods Biomech. Biomed. Eng. 16, 50–51.